FLOW AND HEAT TRANSFER OF MHD GRAPHENE OXIDE-WATER NANOFLUID BETWEEN TWO NON-PARALLEL WALLS

Mohammadreza AZIMI, Rouzbeh RIAZI[*]

Faculty of New Sciences and Technologies, University of Tehran, Tehran, Iran.
[*] rouzbehriazi@yahoo.com

The steady two-dimensional heat transfer and flow between two non-parallel walls of a graphene-oxide nanofluid in presence of uniform magnetic field are investigated in this paper. The analytical solution of the nonlinear problem is obtained by Galerkin Optimal Homotopy Asymptotic Method (GOHAM). At first a similarity transformation is used to reduce the partial differential equations modeling the flow and heat transfer to ordinary nonlinear differential equation systems containing the semi angle between the plates parameter, Reynolds number, the magnetic field strength, nanoparticle volume fraction, Eckert and Prandtl numbers. Finally the obtained analytical results have been compared with results achieved from previous works in some cases.

Key words: "Heat Transfer Enhancement", "Graphene Oxide-Water", "Nanofluid", "Jeffery Hamel Flow", "GOHAM".

1. Introduction

The term nanofluid was envisioned to describe a fluid in which nanometer-sized particles were suspended in conventional heat transfer basic fluids. Nanotechnology aims to manipulate the structure of the matter at the molecular level with the goal for innovation in virtually every industry and public endeavor including biological sciences, physical sciences, electronics cooling, transportation, the environment and national security [1, 2].

Magnetohydrodynamics (MHD) is the study of the interaction of electrically conducting fluids and electromagnetic forces. The field of MHD was initiated by Swedish physicist, Hannes Alfvén for which he received in 1970 the Nobel Prize [3]. The official birth of incompressible fluid magnetohydrodynamics is 1936–1937. In 1937, Hartmann [4] studied the influence of a transverse uniform magnetic field on the flow of a viscous incompressible electrically conducting fluid between two infinite parallel stationary and insulating plates.

Graphene was found to display high quality electron transport at room temperature. Theoretical study was performed on determination of thermal conductivity of graphene and suggests that it has unusual thermal conductivity [5].

Rashidi et al. [6] considered the analysis of the second law of thermodynamics applied to an electrically conducting incompressible nanofluid fluid flowing over a porous rotating disk. They concluded that using magnetic rotating disk drives has important applications in heat transfer enhancement in renewable energy systems. Ellahi [7] studied the magnetohydrodynamic (MHD) flow of non-Newtonian nanofluid in a pipe. He observed that the MHD parameter decreases the fluid motion and the velocity profile is larger than that of temperature profile even in the presence of variable viscosities.

Sheikholeslami and Abelman [8] used two phase simulation of nanofluid flow and heat transfer in an annulus in the presence of an axial magnetic field. Sheikholeslami and Rashidi [9] studied the effect space dependent magnetic field on free convection of Fe_3O_4-water nanofluid. They showed that Nusselt number decreases with increase of Lorentz forces. Sheikholeslami et al. [10] applied LBM to simulate three dimensional nanofluid flow and heat transfer in presence of magnetic field. They indicated that adding magnetic field leads to decrease in rate of heat transfer. Sheikholeslami Kandelousi [11] studied the effect of spatially variable magnetic field on ferrofluid flow and heat transfer considering constant heat flux boundary condition. He found that enhancement in heat transfer decreases with increase of Rayleigh number and Magnetic number but it increases with increase of Hartmann number. Theoretical study of steady flow of an electrically conducting fluid in channels of varying width finds applications in engineering and biological systems, e.g. control of liquid metal flows, crystal growth, design of medical diagnostic devices which make use of the interaction of magnetic fields with tissue fluids, etc [12].

The incompressible viscous fluid flow through convergent and divergent channels is one of the most applicable cases in fluid mechanics, electrical and bio mechanical engineering. One of the most significant examples of Jeffery Hamel problems are those subjected to an applied magnetic field. The MHD systems are used effectively in many applications including power generators, pumps, accelerators, electrostatic filters, droplet filters, the design of heat exchangers, the cooling of reactors etc. The investigation on MHD fluid flow was the main purpose of many pervious researches [13, 14].

In the heart of all the different engineering sciences, everything shows itself in the mathematical relation that most of these problems and phenomena are modeled by ordinary or partial differential equations. In most cases, scientific problems are inherently of nonlinearity that does not admit exact solution, so these equations should be solved using special techniques. Some of these methods are Homotopy Perturbation Method (HPM) [15], Reconstruction of Variational Iteration Method (RVIM) [16], Glerkin Optimal Homotopy Asymptotic Method (GOHAM) [17] and others [18, 19].

The aim of this study is to investigate the velocity profile in MHD Jeffery Hamel flow with nanoparticles by using GOHAM. The obtained approximate result will be compared to numerical solution in numerical case.

2. Mathematical Formulation

For an analytical study of Jeffery–Hamel MHD flows, we consider the two-dimensional flow of a viscous, incompressible and electrically conducting fluid in the presence of a homogeneous magnetic field which acts transversely to the flow (figure.1).

As it can be seen in figure.1 the steady two- dimensional flow of an incompressible conducting viscous fluid from a source or sink at the intersection between two non parallel plane walls is considered. We assume that the velocity is purely radial and depends on r and θ only. The mass, momentum and energy equations in polar coordinates are:

$$\frac{\rho_{nf}}{r} \frac{\partial \left(ru(r,\theta)\right)}{\partial r} \left(ru(r,\theta)\right) = 0 \tag{1}$$

$$u(r,\theta)\frac{\partial u(r,\theta)}{\partial r} = +v_{nf}\left(\frac{\partial^2 u(r,\theta)}{\partial r^2} + \frac{1}{r}\frac{\partial u(r,\theta)}{\partial r} + \frac{1}{r^2}\frac{\partial^2 u(r,\theta)}{\partial \theta^2} - \frac{u(r,\theta)}{r^2}\right) \qquad (2)$$

$$-\frac{1}{\rho_{nf}}\frac{\partial P}{\partial r} - \frac{\sigma B_0^2}{\rho_{nf}r^2}u(r,\theta)$$

$$-\frac{1}{\rho_{nf}r}\frac{\partial P}{\partial \theta} + \frac{2\mu_{nf}}{\rho_{nf}r^2}\frac{\partial u(r,\theta)}{\partial \theta} = 0 \qquad (3)$$

$$u(r,\theta)\frac{\partial T(r,\theta)}{\partial r} = \alpha_{nf}\left(\frac{\partial^2 T(r,\theta)}{\partial r^2} + \frac{1}{r}\frac{\partial T(r,\theta)}{\partial r} + \frac{1}{r^2}\frac{\partial^2 T(r,\theta)}{\partial \theta^2}\right) \qquad (4)$$

$$+\frac{\mu_{nf}}{(\rho C_p)_{nf}}\left(4\left(\frac{\partial u(r,\theta)}{\partial r}\right) + \frac{1}{r^2}\left(\frac{\partial u(r,\theta)}{\partial \theta}\right)^2\right)$$

Since we have a symmetric geometry, the boundary conditions will be:

$$\left(\frac{\partial u(r,\theta)}{\partial r}\right) = 0, \quad \frac{\partial T(r,\theta)}{\partial \theta} = 0, \quad u(r,\theta) = 0 \quad \left(At \quad the \quad Channel \quad Centerline\right) \qquad (5)$$

$$T = T_w, \quad u(r,\theta) = 0 \quad \left(At \quad the \quad Plates\right)$$

Here B_0 is the electromagnetic induction, $u(r)$ is the velocity along radial direction, P is the fluid pressure, σ is the conductivity of the fluid, ρ_{nf} is the density of fluid and v_{nf} is the coefficient of kinematic viscosity. By introducing φ as a solid volume fraction, fluid density, dynamic viscosity, the kinematic viscosity [16], thermal diffusivity and thermal conductivity [17] of nanofluid can be written as follows:

$$\begin{cases} \rho_{nf} = \rho_f(1-\varphi) + \rho_s\varphi \\[2mm] \mu_{nf} = \dfrac{\mu_f}{(1-\varphi)^{2.5}} \\[2mm] v_{nf} = \dfrac{\mu_f}{\rho_{nf}} \\[2mm] \alpha_{nf} = \dfrac{k_{nf}}{(\rho C_p)_{nf}} \\[2mm] \dfrac{k_{nf}}{k_f} = \dfrac{(k_s + 2k_f) - 2\varphi(k_s - k_f)}{(k_s + 2k_f) + \varphi(k_s - k_f)} \end{cases} \qquad (6)$$
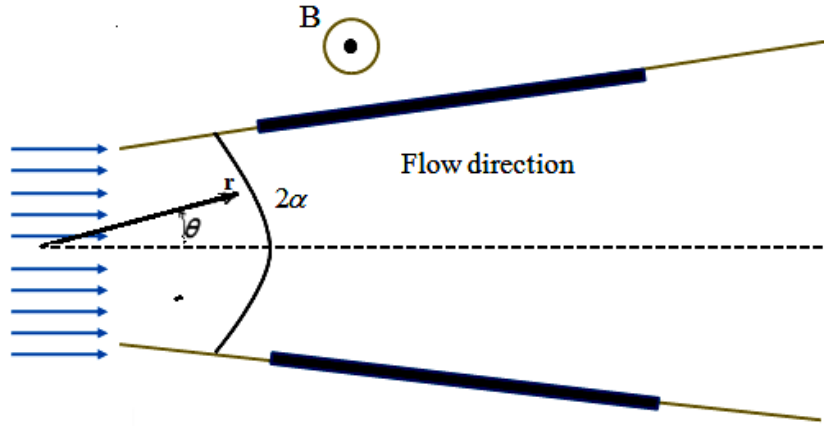
Fig. 1. Geometry of problem.

Using $\eta = \dfrac{\theta}{\alpha}$ as the semi angle between walls, the dimensionless form of the velocity parameter can be yield by dividing that to its maximum values as $f(\eta) = \dfrac{f(\theta)}{f_{max}}$ where $f_{max} = rU$. Introducing $\zeta = \dfrac{T}{T_w}$, substituting dimensionless parameters into equations.1-5 and eliminating the pressure term implies the following nonlinear third order boundary value problems:

$$f''' + 2\alpha \, \mathrm{Re}\left[\left((1-\phi) + \frac{\rho_s}{\rho_f}\phi\right)(1-\phi)^{2.5}\right]ff' + \left(4 - (1-\phi)^{1.25}H\right)\alpha^2 f' = 0 \tag{7}$$

$$\frac{1}{\left[1 - \varphi + \varphi\dfrac{(\rho C_p)_s}{(\rho C_p)_f}\right]}\left[\frac{k_{nf}}{k_f}\zeta'' + \frac{\mathrm{Pr}\,Ec}{(1-\varphi)^{2.5}}\left(4\alpha^2 f^2 + f'^2\right)\right] = 0 \tag{8}$$

Where $\mathrm{Pr} = \dfrac{\mu_f (C_p)_f}{k_f}$ is the Prandtl number, $\mathrm{Re} = \dfrac{\alpha U_{max}}{v}$ is a Reynolds number, $\mathrm{Pr} = \dfrac{U^2}{(C_p)_f T_w}$ is Eckert number and $H = \sqrt{\dfrac{\sigma B_0^2}{\rho v}}$ is the Hartmann number.

With the following boundary conditions:

$$f(0) = 1, \ f(1) = 0, \ f'(0) = 0, \ \zeta(1) = 1, \ \zeta'(0) = 0 \tag{9}$$

In the limit of $\alpha = 0$, the flow becomes that of plane Poiseuille flow between two parallel plates. Physical quantities of interest are the skin friction coefficient, local Nusselt number, heat transfer rate and shear stress which are defined as:

$$c_f = \frac{\tau_w}{\rho_f U^2}, \quad Nu = \frac{r q_w|_{\theta=\alpha}}{k_f T_w}, \quad q_w = -k_{nf}\nabla T, \quad \tau_w = \mu_{nf}\left(\frac{1}{r}\left(\frac{\partial u(r,\theta)}{\partial \theta}\right)\right) \tag{10}$$

substitution of equation.10 into equations. 7 and 8, gives:

$$c_f = \frac{1}{Re(1-\varphi)^{2.5}} f'(1), \quad Nu = -\frac{1}{\alpha} \frac{k_{nf}}{k_f} \zeta'(1) \tag{11}$$

3. Application of GOHAM

Following differential equation is considered:

$$L(u(t)) + N(u(t)) + g(t) = 0, \quad B(u) = 0 \tag{12}$$

Where L is a linear operator, $u(t)$ is an unknown function, $g(t)$ is a known function, $N(u(t))$ is a nonlinear operator and B is a boundary operator. By means of OHAM one first constructs a set of equations:

$$(1-p)[L(\phi(\tau,p) + g(\tau))] - H(p)[L(\phi(\tau,p)) + g(\tau) + N(\phi(\tau,p))]B(\phi(\tau,p)) = 0 \tag{13}$$

Where τ is an independent variable, $p \in [0,1]$ is an embedding parameter, $H(p)$ denotes a nonzero auxiliary function for $p \neq 0$ and $H(0) = 0$, $\phi(\tau,p)$ is an unknown function. Obviously, when $p = 0$ and $p = 1$, it holds that:

$$\phi(\tau,0) = u_0(\tau), \quad \phi(\tau,1) = u(\tau) \tag{14}$$

Thus, as p increases from 0 to 1, the solution $\phi(\tau,p)$ varies from $u_0(\tau)$ to the solution $u(\tau)$, where $u_0(\tau)$ is obtained from Eq. (14) for $p = 0$:

$$L(u_0(\tau)) + g(\tau) = 0, \quad B(u_0) = 0 \tag{15}$$

The auxiliary function $H(p)$ can be chosen in the form:

$$H(p) = p_1 C_1 + p_2 C_2 + \cdots \tag{16}$$

Where C_1, C_2 , … are constants which can be determined later. Expanding $\phi(\tau,p)$ in a series with respect to p, one has:

$$\phi(\tau,p,C_i) = u_0(\tau) + \sum_{k>1} u_k(\tau,C_i)p_k, \quad i = 1,2,... \tag{17}$$

Substituting equation.16 into equation.13, collecting the same powers of p, and equating each coefficient of p to zero, we obtain set of differential equation with boundary conditions. Solving differential equations by boundary conditions $u_0(\tau), u_1(\tau,C_1), u_2(\tau,C_2),...$ are obtained. Generally speaking, the solution of equations. 7, 8 can be determined approximately in the form:

$$\phi(\tau,p,C_i) = u_0(\tau) + \sum_{k>1} u_k(\tau,C_i)p_k, \quad i = 1,2,... \tag{18}$$

$$\tilde{u}(m) = u_0(\tau) + \sum_{k=1}^{m} u_k(\tau,C_i) \tag{19}$$

Note that the last coefficient C_m can be function of τ. Substituting Equation.19 into Equation.12, there results the following residual:

$$R(\tau,C_i) = L(\tilde{u}^{(m)}(\tau,C_i)) + g(\tau) + N(\tilde{u}^{(m)}(\tau,C_i)) \tag{20}$$

If $R(\tau,C_i) = 0$ then $\tilde{u}^{(m)}(\tau,C_i)$ happens to be the exact solution. Generally such a case will not arise for nonlinear problems, but the functional by Galerkin method can be minimized:

$$w_i = \frac{\partial R(\tau, C_1, C_2, \cdots, C_m)}{\partial C_i}, \quad i = 1, 2, \ldots, m \tag{21}$$

The unknown constants C_i ($i = 1, 2, \ldots, m$) can be identified from the conditions:

$$J(C_1, C_2) = \int_a^b w_i R(\tau, C_1, C_2, \ldots, C_m) d\tau = 0 \tag{22}$$

Where a and b are two values, depending on the given problem. With these constants, the approximate solution (of order m) (Equation. (22)) is well determined. It can be observed that the method proposed in this work generalizes these two methods using the special (more general) auxiliary function $H(p)$.

4. Results and Discussions

The problem of MHD flow of nanofluid is associated with various kinds of dimensionless parameters due to its multiphysics nature. In this section, we will also discuss about the obtained results of Graphene Oxide-water nanofluid flow between converging-diverging plates for various solid volume fraction, Eckert, Reynolds and Hartman number. The physical properties of GO- water nanofluid are tabulated in Table.1.

Table1. Thermo physical properties of water and GO nanoparticle [16].

	$\rho(kg/m^3)$	$C_p(j/kgk)$	$k(W/m.k)$
Pure water	997.1	4179	0.613
Graphene Oxide	1800	717	5000

Figure.2-a shows the effect of increasing Reynolds numbers on the fluid velocity for fixed Hartmann numbers when $\alpha = \pi/9$, $\varphi = 0.2$, $H = 300$. As it can be illustrated in figure.2-a Back flow is possible for large Reynolds numbers in the case of diverging channels.

The effect of Hartmann number for a diverging channel is demonstrated in figure.2-b. The velocity curves show that the rate of momentum transport is considerably reduced with increase of Hartmann number.
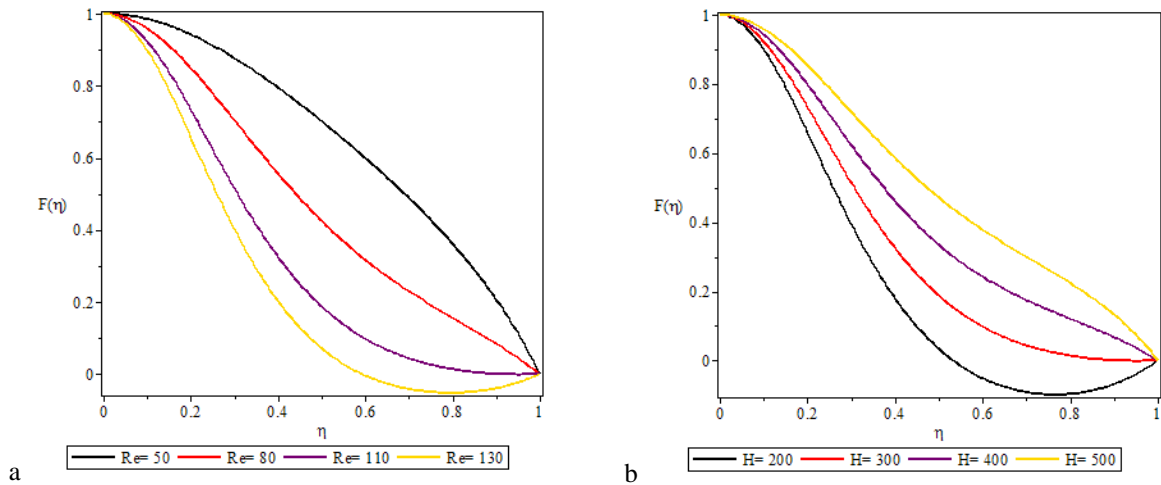

a   b

Figure.2. Effect of Reynolds and Hartmann numbers on velocity profile when $\alpha = \pi/9$ $\varphi = 0.2$, a- $H = 300$ and b- $Re = 110$

This clearly indicates that the transverse magnetic field opposes the transport phenomena. Because the that variation of Ha leads to the variation of the Lorentz force due to magnetic field and the Lorentz force produces more resistance to transport phenomena.

Nano solid volume fraction plays key role and it has significant effect on both velocity and temperature components. Figure.3 illustrates the effect of solid volume fraction of graphene oxide nanoparticle on temperature profile in case $H = 400$, $R = 110$,

$Ec = 0.2$, $\Pr = 7$, $\alpha = \frac{\pi}{12}$.

The increase in GO-nanoparticles volume fraction tends to increase the dimensionless temperatures due to increase in heat transfer. For energy applications of nanofluids, two remarkable properties of nanofluids are utilized, one is the higher thermal conductivities of nanofluids, enhancing the heat transfer, and another is the absorption properties of nanofluids. In this study, the absorption properties of GO-Water nanofluid are considered negligible.
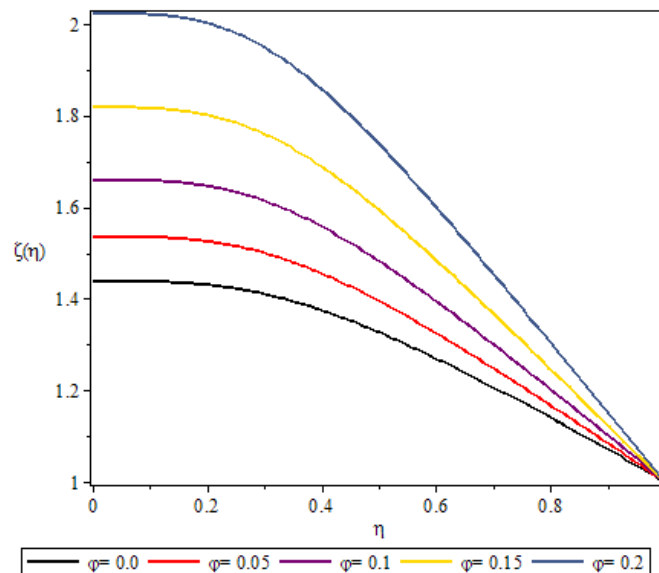

Figure.3. Effect of Nanoparticle solid volume fraction on temperature profile in case

$H = 400$, $R = 110$, $Ec = 0.2$, $\Pr = 7$, $\alpha = \frac{\pi}{12}$.

The effect of semi angle between nonparallel walls on non-dimensional temperature of the nanofluid is investigated through figure.4 for convergent channel when the other non dimensional parameters are kept fixed in $H = 300$, $R = 70$, $Ec = 0.1$, $\Pr = 7$, $\varphi = 0.1$. This figure describe that the temperature is increasing function of α in convergent channels.
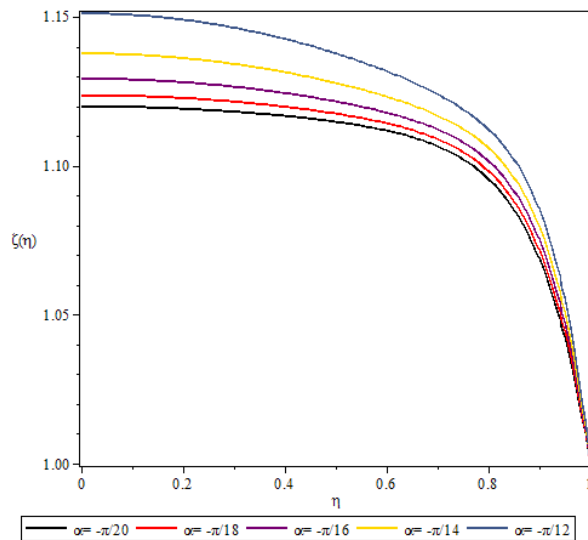
Figure.4.Effect of angle between plates on temperature profile when $H = 300$, $R = 70$, $Ec = 0.1$, $\Pr = 7$, $\varphi = 0.1$ for converging channel .

The effect of semi angle between nonparallel walls on velocity profile of the nanofluid is investigated through figure.5-a, b for both convergent and divergent channel in case $\varphi = 0.2$, $H = 400$, $\mathrm{Re} = 50$.
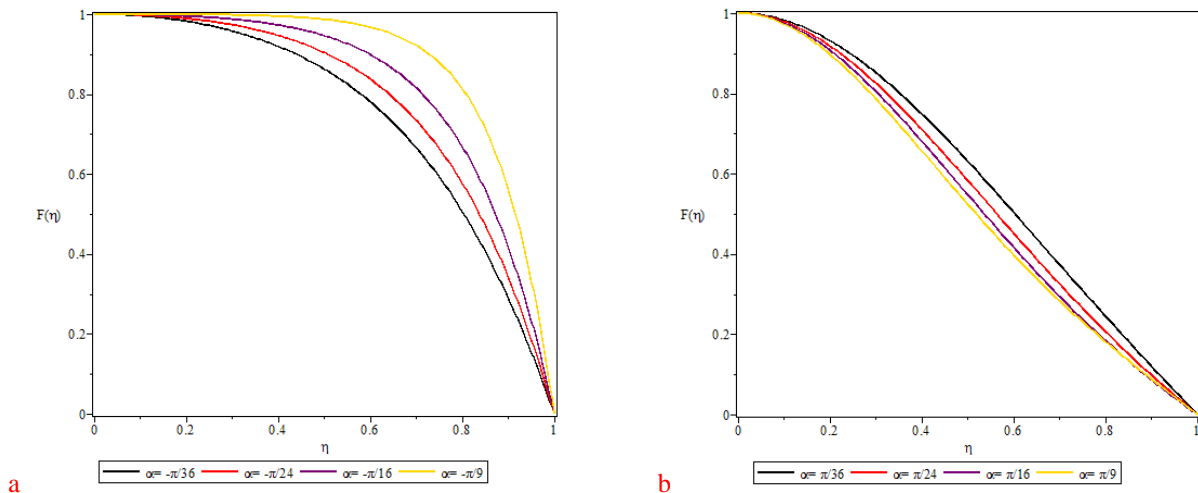

Figure.5. Effect of semi angle between walls on velocity profile when $\varphi = 0.2$, $H = 400$, $\mathrm{Re} = 50$ a-convergent channel and b- divergent channel.

Impact of Eckert number and Hartmann number on temperature profiles are display in figure.6 a and b, respectively. Figure. 5 confirm that when Eckert number increases, temperature profiles increase whereas increasing Hartmann number reduce velocity values. This is in line with the physics of the system in that because of the higher thermal conductivity at higher Ec numbers, higher values of thermal diffusivity can be observed.

Another consequence which can be achieved from figure.6 is that, by changing the value of H from 100 to 200, Temperature on wall is decreased from 1.18 to 1.13. Such an effect even becomes less sensible at higher values of H. Also, it shows that increasing Eckert number leads to increasing the curve of presented surface when H is constant.
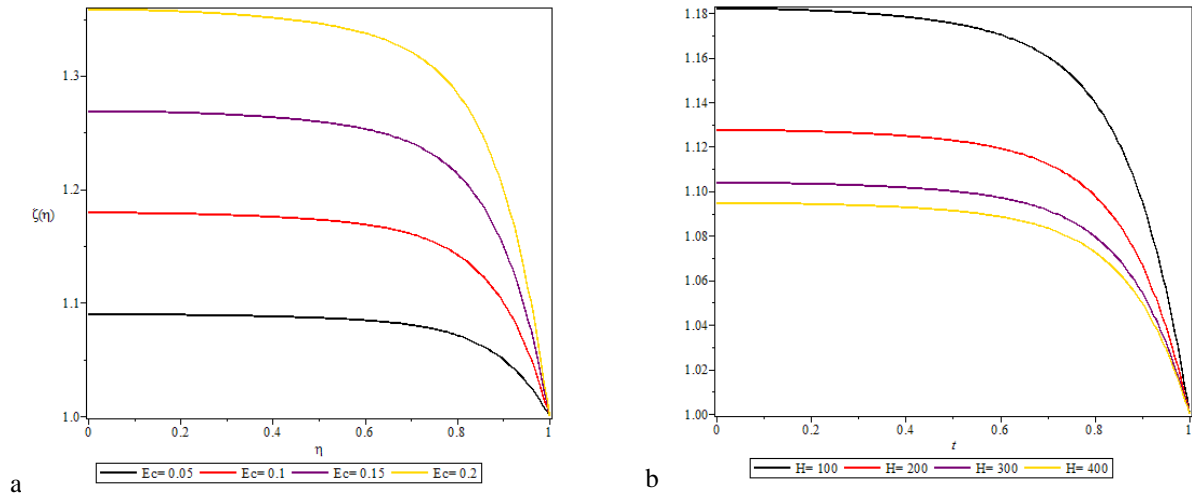
Figure.6. Effect of Eckert and Hartmann numbers on temperature profile when

$$\alpha = -\frac{\pi}{24} \quad Re = 70, \quad Pr = 7, \quad \varphi = 0.1, \text{ a- } H = 400 \quad \text{and b- } Ec = 0.05$$

The variations in the skin friction coefficient and the Nusselt number with the governing parameters are presented in table.2 and 3, respectively. According to the performed calculations (equation.5) and table.2, one can thoroughly consider that generally, adding nanoparticles to the working fluid results in an increase in the value of Nu. By increasing the value of nanoparticles volume fraction, the heat transfer rate raises.

Table.2. Nusselt number in case $H = 50$ and $\alpha = 15^0$.

Solid Volume Fraction	Eckert Number	Reynolds Number	Nusselt Number
0.1	0.1	50	4.9010
0.2			7.0706
0.1	0.2		9.8024
0.2			14.141
0.1	0.1	100	9.4166
0.2			13.8571
0.1	0.2		18.8331
0.2			27.713

Effects of Angle of the channel, Reynolds number and Hartmann number on Skin friction coefficient is shown in table. 3. Skin friction coefficient is an increasing function of Reynolds number and opening angle but decease function of Hartmann number.

Table.3. Skin friction coefficient in case $\varphi = 0.15$.

Angle Between Plates	Hartmann Number	Reynolds Number	Skin Friction Coefficient
5 degree	50	25	-0.1771
10 degree			-0.2173
5 degree	100		-0.1802
10 degree			-0.2282
5 degree	50	50	-0.1049
10 degree			-0.1377
5 degree	100		-0.1063
10 degree			-0.1424

Interestingly, it is not clearly evident to out rightly predict the effects of the different Eckert number values on Nusselt number. This may be because of the complications of the proposed model. Nevertheless, the present study provided a good base for further research.

Table.4 shows a comparison between GOHAM solution and ADM solution [20] for velocity when $H = 250,\ \mathrm{Re} = 25,\ \alpha = 5\ \ \phi = 0$.

Table.4. Comparison between DTM solution and ADM solution [20] when $H = 250$, $\mathrm{Re} = 25$, $\alpha = 5$, $\phi = 0$

η	GOHAM	ADM [14]	Error
0	1.000000	1.000000	0.000
0.2	0.954700	0.960841	0.007
0.4	0.821345	0.811225	0.012
0.6	0.614891	0.604866	0.009
0.8	0.339890	0.325834	0.014
1	0.000000	0.000000	0.000

Conclusions

This investigation deals with the analysis of heat transfer and MHD viscous Graphene oxide water nanofluid flow between two non-parallel walls for both converging/ diverging cases.

Based on achieved results, an increase in the magnetic field intensity was found to have a strong stabilizing effect on the results for both diverging and converging channel geometries.

The results show that the non-dimensional parameters have a strong influence on the temperature profile. The main findings are summarized as follows:

- The thickness of thermal boundary layer decreases with increment in solid volume fraction of nanofluid due to higher heat transfer.

- Nusselt number is an increasing function of Reynolds number, solid volume fraction and Eckert number.

- Skin friction coefficient is an increasing function of Reynolds number and opening angle but decease function of Hartmann number.

- The comparison between analytical results and results achieved by pervious researches revealed that GOHAM can be simple, powerful and efficient techniques for finding analytical solutions in science and engineering non-linear differential equations.

Nomenclature

B_0	Magnetic field(wb.m^{-2})		θ	Any angle
Ec	Eckert number			
$f(\eta)$	Dimensionless velocity		ρ	Density
Ha	Hartmann number		ϕ	Nanoparticle volume fraction
P	Pressure term		μ	Dynamic viscosity
Pr	Prandtl number			
Re	Reynolds number		υ	Kinematic viscosity
			ζ	Dimensionless temperature
r, θ	Cylindrical coordinates		β	Constant
T	Temperature			
T_w	Wall temperature			
U_{max}	Maximum value of velocity		*Subscripts*	
u, v	Velocity components along x, y axes, respectively		∞	Condition at infinity
B_0	Magnetic field(wb.m^{-2})		Nanofluid	nf
Greek symbols			Base fluid	f
α	Angle of the channel		s	Nano-solid-particles
η	Dimensionless angle			

References

[1] Mahian, O., et al., A review of the applications of nanofluids in solar energy, *Int. J. Heat Mass Transfer*, *57* (2013), pp.582–594.

[2] Cimpean, D. S., Pop, I., Fully developed mixed convection flow of a nanofluid through an inclined channel filled with a porous medium, *Int. J. Heat Mass Transfer*, *55* (2012), pp.907–914.

[3] Alfvén, H., Existence of electromagnetic-hydrodynamic waves, *Nature*, *150* (1942), pp.405-406.

[4] Hartmann, J., *Hg-Dynamics I.: Theory of the laminar flow of an electrically conducting liquid in a homogeneous magnetic field*, Levin & Munksgaard, Ejnar Munksgaard, 1937.

[5] Saito, K., et al., Ballistic thermal conductance of a graphene sheet, *Phys. Rev. B: Condens Matter*, *76* (2007), ARTICLE ID: 115409.

[6] Rashidi, M. M., et al., Entropy generation in steady MHD flow due to a rotating porous disk in a nanofluid, *Int. J. Heat Mass Transfer*, *62* (2013), pp.515–525.

[7] Ellahi, R., The effects of MHD and temperature dependent viscosity on the flow of non-Newtonian nanofluid in a pipe: Analytical solutions, *Appl. Math. Model., 37* (2013), 3, pp.1451-1467.

[8] Sheikholeslami, M., Abelman, S., Two phase simulation of nanofluid flow and heat transfer in an annulus in the presence of an axial magnetic field, *IEEE Transactions on Nanotechnology*, *14* (2015), 3, pp.561-568, DOI:10.1109/TNANO.2015.2416318.

[9] Sheikholeslami, M., Rashidi, M. M., Effect of space dependent magnetic field on free convection of Fe3O4-water nanofluid, *J. Taiwan. Inst. Chem. E*, (2015), DOI: 10.1016/j.jtice.2015.03.035.

[10] Sheikholeslami, M., et al., Lattice Boltzmann Method for simulation of magnetic field effect on hydrothermal behavior of nanofluid in a cubic cavity, *Physica A: Statistical Mechanics and its Applications*, *432* (2015), pp.58-70.

[11] Sheikholeslami Kandelousi, M., Effect of spatially variable magnetic field on ferrofluid flow and heat transfer considering constant heat flux boundary condition, *Eur. Phys. J. Plus., 129* (2014), pp.248-260.

[12] Sheikholeslami, M., et al., Investigation of Nanofluid Flow and Heat Transfer in Presence of Magnetic Field Using KKL Model, *Arab. J. Sci. Eng., 39* (2014), pp.5007-5016.

[13] Raftari, B., Yildirim, A., The application of homotopy perturbation method for MHD flows of UCM fluids above porous stretching sheets, *Comp. Math. Appl., 59* (2010), pp.3328_3337.

[14] Ganji, D. D., Azimi, M., Application of DTM on MHD Jeffery Hamel Problem with Nanoparticles, *U.P.B. Scientific Bulletin: D*, *75* (2013), 1, pp. 223-230.

[15] Ganji, D. D., et al., Determination of Temperature Distribution for Annular Fins with Temperature Dependent Thermal Conductivity by HPM, Thermal Science, 15 (2011), 1, pp. 111-115.

[16] Azimi, A., Azimi, M., Analytical Investigation on 2-D unsteady MHD Viscoelastic flow between Moving Parallel Plates Using RVIM and HPM, *Walailak J. Sci. & Tech. 11* (2014), 11, pp.955-963.

[17] Azimi, M., et al., Investigation of the Unsteady Graphene Oxide Nanofluid Flow Between Two Moving Plates, *J. Comput. Theor. NanoScie. 11* (2014), pp.2104-2108.

[18] Ganji, D. D., Azimi, M., Application of Max min Approach and Amplitude Frequency Formulation to the nonlinear oscillation systems, *U.P.B. Scientific Bulletin: A 74* (2012), 3, pp.131-140.

[19] Ganji, D. D., et al., Energy Balance Method and amplitude frequency formulation based of strongly nonlinear oscillator, *Indian J. Pure Ap. Mat. 50* (2012), pp.670-675.

[20] Sheikholeslami, M., et al., Analytical Investigation of Jeffery Hamel flow with High Magnetic Field and nanoparticle by Adomian Decomposition Method, *App. Math Mech. –Engl. Ed*, *33* (2012), 1, pp.25-36.